TSINGHUA SCIENCE AND TECHNOLOGY
ISSN 1007-0214 08/14 pp511–524
DOI: 10.26599/TST.2022.9010015
Volume 28, Number 3, June 2023

An ANN-Based Short-Term Temperature Forecast Model for Mass Concrete Cooling Control

Ming Li, Peng Lin*, Daoxiang Chen, Zichang Li, Ke Liu, and Yaosheng Tan

Abstract: Concrete temperature control during dam construction (e.g., concrete placement and curing) is important for cracking prevention. In this study, a short-term temperature forecast model for mass concrete cooling control is developed using artificial neural networks (ANN). The development workflow for the forecast model consists of data integration, data preprocessing, model construction, and model application. More than 80 000 monitoring samples are collected by the developed intelligent cooling control system in the Baihetan Arch Dam, which is the largest hydropower project in the world under construction. Machine learning algorithms, including ANN, support vector machines, long short-term memory networks, and decision tree structures, are compared in temperature prediction, and the ANN is determined to be the best for the forecast model. Furthermore, an ANN framework with two hidden layers is determined to forecast concrete temperature at intervals of one day. The root mean square error of the forecast precision is 0.15 ℃ on average. The application on concrete blocks verifies that the developed ANN-based forecast model can be used for intelligent cooling control during mass concrete construction.

Key words: artificial neural networks (ANN); predictive modeling; temperature forecast; mass concrete; cooling control

1 Introduction

Since the 1990s, several 300-meter-level high arch dams, such as Xiaowan, JinPing I, Xiluodu, Wudongde, and Baihetan dams have been or are being constructed in China[1–3]. New features associated with these mass structures, such as large block sizes, limited placement space, and tight construction schedules, increase the difficulty of concrete temperature control during placement and curing stages. This increases the risk of thermal cracking on the dams, resulting in safety concerns. With the aim to prevent thermal cracking in mass concrete, control measures have been implemented in dam design and construction[4, 5], including concrete design optimization, block slitting design, concrete skip placing, fresh concrete insulation, pipe cooling, and hydration moisture retention. For pipe cooling, operation and cooling parameters are adjusted manually based on past experiences but now can be remotely and automatically operated via recent proportional-integral-derivative control algorithms[6]. However, temperature control is still lagging. If concrete temperatures can be forecast precisely and timely, cooling control strategies can be developed and implemented simultaneously, which leads to further improvements.

Numerical simulation, statistical analysis, and data mining are typical methods adopted for concrete temperature forecasts. In numerical simulations, thermodynamic equations require complex calculations and complex analytical procedures. Statistical analysis provides best-fit results but lacks precision. The coupling

• Ming Li, Peng Lin, and Daoxiang Chen are with the Department of Hydraulic Engineering, Tsinghua University, Beijing 100084, China. E-mail: l-m19@mails.tsinghua.edu.cn; celinpe@tsinghua.edu.cn; chendx2000@163.com.
• Zichang Li is with the Sichuan Energy Internet Research Institute, Tsinghua University, Chengdu 610213, China. E-mail: changzilee@gmail.com.
• Ke Liu and Yaosheng Tan are with China Three Gorges Construction Engineering Corporation, Chengdu 610000, China. E-mail: 273202798@qq.com; 1244292229@qq.com.
* To whom correspondence should be addressed.
Manuscript received: 2022-02-19; revised: 2022-05-27; accepted: 2022-06-06

of numerical simulation and statistical analysis are costly and time-consuming. With the recent boom of artificial intelligence applied in dam construction[7–9], multiple-source data related to cooling control practices have been accumulated. Mining of these massive data helps develop quick and accurate concrete temperature forecasts. Machine learning algorithms (e.g., support vector machines (SVM), artificial neural networks (ANN), long short-term memory networks (LSTM), and decision tree structures (DT)), and Gray System theory have been applied in forecasting dam construction parameters for deformation analysis[10, 11], concrete performance[12], and leakage flow[13]. However, few studies focus on mass concrete temperature forecasting due to poor cooling monitoring and temperature control technology. Available studies[14–16] simplify the problem and forecast only characteristic concrete temperature parameters, such as the maximum temperature during the early cement hydration age. Recently, rapid intelligent construction of hydropower projects in China has collected multi-source concrete cooling data, which allows for the development of concrete temperature forecasts[9, 16–19].

In the present study, an ANN-based model with two hidden layers is developed for real-time, accurate concrete temperature forecast for mass concrete cooling control. This framework for real-time prediction of concrete temperature at intervals of one day is proposed after reviewing monitoring data collected in the Baihetan Dam. A total of fourteen parameters related to mass concrete design, construction, and cooling are used. Time series data—such as air temperature, cooling water flow, inlet flow temperature, and concrete temperature—are resampled at intervals of one day. The ANN-based forecast model is evaluated with accuracy measures of root mean squared error (RMSE) using a dataset of 87 876 samples. To improve the prediction accuracy, we optimized the quantities of hidden layers, neurons, and algorithms of the ANN-based model. Finally, the trained ANN-based forecast model is compared with models based on other algorithms (e.g., SVM, LSTM, and DT). The remainder of this paper is organized as follows: Section 2 introduces work related to the prediction of mass concrete temperature. Section 3 explains the workflow of the ANN-based model and implementation. Section 4 presents an experiment on a real dam site using data from intelligent cooling control system (ICCS) and compares the error distribution of ANN with that of other machine learning algorithms. Conclusions are presented in Section 5.

2 Literature Review

2.1 Temperature control for mass concrete

Mass concrete is widely used in hydraulics, transportation, construction, and other engineering industries. Thermal cracking in concrete occurs in the early hydration stage due to uneven distribution of stresses resulting from hydration heat and boundary constraints, endangering structural durability and even stability. Thermal cracks may initiate in the outlet, gallery, heel[20], surface, and interior of dam concrete blocks[1, 21], tunnel spillway[22], and overtopping of placed blocks from seasonal low-temperature flooding[23]. Temperature control of mass concrete in the construction period (e.g., concrete placement and curing) has received extensive attention in related academics and industries. The temperature distribution in concrete can be affected by concrete mix design proportions, cement hydration heat, casting block sizes[24], casting, cooling measures[25, 26], ambient temperature[27], wind speed[28], surface insulation, and other factors.

Pipe cooling is one of the most widely used measures for exchanging internal hydration heat, controlling temperature rise (or drop), and avoiding cracking during mass concrete construction. Cooling flow rates and water temperatures affect how concrete temperature changes. In 1931, the United States Bureau of Reclamation carried out the first experiment of concrete cooling at the Owyhee Arch Dam in Oregon. Two years later, the water cooling method was fully applied in the construction of the Hoover Dam, achieving satisfactory temperature control. Since then, water cooling has been widely used in the construction of concrete dams and other mass structures[22].

In the past ten years, concrete cooling operations have shifted from manual to digital and further to intelligent control. Lin et al.[29] developed a comprehensive Intelligent Cooling Control System Version 1.0 (ICCS 1.0) to monitor the cooling operation in the construction of the Xiluodu Dam in China. Temperature field reconstruction methods and intelligent control algorithms were later integrated into the ICCS 2.0[30, 31], which was successfully applied in the Wudongde Dam and the Baihetan Dam in China. The ICCS 2.0 can conduct real-time monitoring and control of various parameters, including inner concrete temperature, ambient temperature, cooling flow rate, and inlet water temperature. In the present study, an

ANN-based short-term temperature forecast model for mass concrete cooling control was developed using the monitoring data collected by the ICCS 2.0 in the Baihetan Dam. The ICCS 2.0 continuously collected time-based parameter series of the temperature, cooling flow, inlet temperature, and air temperature of each concrete block at a frequency of 2.5 min (150 s). By combining the cooling dataset with the design- and construction-related parameters of each concrete block, the dataset was obtained for developing the short-term temperature forecast model.

2.2 Prediction methods

Current methods for concrete temperature prediction can be divided into three categories: Numerical simulation, statistical analysis, and data mining. Table 1 summarizes the features of these methods.

In numerical simulations, concrete temperature prediction is based on the Fourier's Law of thermal conduction and associated heat conduction differential equation system with internal heat sources. By modeling the layered concrete placement and cement hydration heat, the time history of the concrete temperature field was recreated. As commercial software, such as ANSYS, MIDAS, and SapTis, becomes available, temperature field modeling continues to be improved. Numerical simulation is widely applied in designing various mass concrete structures, such as concrete dams[32] and bridge anchor blocks[33], owing to its high accuracy. In recent years, more factors are incorporated into the numerical simulation, such as concrete microstructure[32], climate data[33], concrete maturity[34], concrete cooling[35], and crack propagation[36]. These additions have further improved the accuracy of temperature field prediction. However, numerical simulation also has disadvantages, such as complex model setups, huge calculation efforts, and long computation running times. These issues lead to difficulties in meeting the needs for real-time prediction for concrete temperature control.

Statistical analyses—such as data regression[37–40] and autoregressive integrated moving average (ARIMA)[41]—of historical monitoring data can be used to develop best-fit models (i.e., equations or formulas) for predicting concrete temperature changes in similar scenarios. This simple and rapid method is widely used in dams[37], bridges[38, 40], and other concrete structures. For periodic temperature prediction, the ARIMA can also be used to develop prediction models[41]. Nevertheless, for problems with big data, numerous influencing factors, or complex mapping relationships, statistics-based predictive modeling can only be used to obtain proximation or inaccurate results due to problem simplifications.

Data mining was developed in the late 1980s. Also known as knowledge extraction, knowledge discovery in databases, data fishing, data archaeology, information harvesting, or business intelligence, data mining is an interdisciplinary subject that integrates database technology, artificial intelligence, machine learning, statistics, and data visualization. Analysis of large amounts of data can reveal meaningful relationships, trends, or patterns between different parameters. One of the core functions of data mining technology is prediction, including regression and classification. Concrete temperature prediction is a typical regression task. Prediction models based on machine learning algorithms can be divided into three types. (1) Prediction models based on a single algorithm. Machine learning algorithms such as logistic regression (LR), support vector regression (SVR), ANN, DT, convolutional neural network (CNN), gradient boosting machine, and LSTM[42] are widely applied predictions of temperature, prices, and other factors. For example, CNN-based models were proposed to forecast long-term strains in concrete structures[12]. Comparing dam deformation prediction, Li[43] found that the effect of ANN is better than multiple linear regression for complex and highly-nonlinear problems. (2) Prediction models based on the composition of several machine learning algorithm layers. CNN performs well on spatial data, and LSTM is good at dealing with time-series data. To take advantage of the feasures of different algorithms, researchers

Table 1 Comparison of concrete temperature prediction methods.

Method	Fundamental theory	Accuracy	Complexity	Reliability	Efficiency
Numerical simulation	Fourier's Law	High	Complex modeling	High	Time-consuming
Statistical analysis	Multiple regression, ARIMA, ...	Low	Easy to implement	Low	Timely
Data mining	Machine learning algorithms	High, affected by data quality	Relatively complex in data preprocessing	Medium, nondeterministic	Timely when predicting

have widely explored the approach of sequential and parallel layers. CNN-LSTM models are proposed for forecasting tasks, such as for gold price time series[44] and horizontal irradiance[45]. Models containing three parallel LSTM layers[46] are applied in taxi demand prediction and showed better accuracy. (3) Ensemble learning prediction models have gained comprehensive attention in recent years, combining several prediction models with preferences to generate predictions with better overall performance. To construct a hybrid ensemble model with higher accuracy in concrete compressive strength prediction, Asteris et al.[47] combined four conventional machine learning models, namely, ANN, Multivariate Adaptive Regression Splines, Gaussian Process Regression, and Minimax Probability Machine Regression. However, few studies focused on real-time temperature forecasting during concrete construction.

Existing methods for concrete temperature prediction can be divided into three categories. (1) Prediction of characteristic temperature values during construction. Cai[48] developed a concrete maximum temperature prediction method based on SVM and ANN algorithms and trained the model with monitoring data collected with 461 thermometers. (2) Prediction of Semi-quantitative concrete temperature. Xie et al.[15] used DT algorithms to predict the change of concrete maximum temperature (e.g., at the center or mid-depth). Song et al.[14] proposed a concrete temperature interval prediction method based on a hybrid-kernel relevance vector machine (HK-RVM) for grouting. (3) Prediction of temperature history. Li[43] established a history prediction model for concrete temperature evolution based on SVM. The input was an 18-dimensional vector, and the output was the concrete temperature at a given time.

As discussed above, current research mainly focuses on the temperature at specific time points or its long-term evolution. Meanwhile, accurate short-term temperature prediction methods to supervise the real-time adjustment operation of concrete temperature control during concrete construction remains lacking.

3 ANN-Based Short-Term Temperature Forecast Model

3.1 Workflow

In this study, ANN is used to develop the proposed short-term forecast model. ANN algorithm is good for fitting problems of high nonlinearity, complex relationships, and/or multiple hidden layers and neurons. Before obtaining a satisfying trained forecast model, data integration, data preprocessing, and model construction must be executed (Fig. 1).

(1) **Data integration.** Short-term concrete temperature changes are affected by different factors, both non-time-series (e.g., material properties, dimension tolerances, and concrete placing plans) and time-series (e.g., water flow, ambient temperature, and inlet flow temperature). The data are typically collected from different sources and in varying formats. In this step, raw data are reviewed by selecting critical parameters and deleting duplicates and are then resampled at the same time interval (e.g., one day) and into the same format.

(2) **Data preprocessing.** Noises such as errors, duplicates, and missing values are filtered out through data preprocessing. The other two sub-steps, namely, normalization and principal component analysis (PCA), further improve the data quality. Samples are formed as an $n+1$ dimensional vector $[x_1, x_2, \ldots, x_n, y]$ for concrete temperature prediction. The first n values are used as the model input. The last value y, which represents the average concrete temperature on the next day, is used for model training and testing.

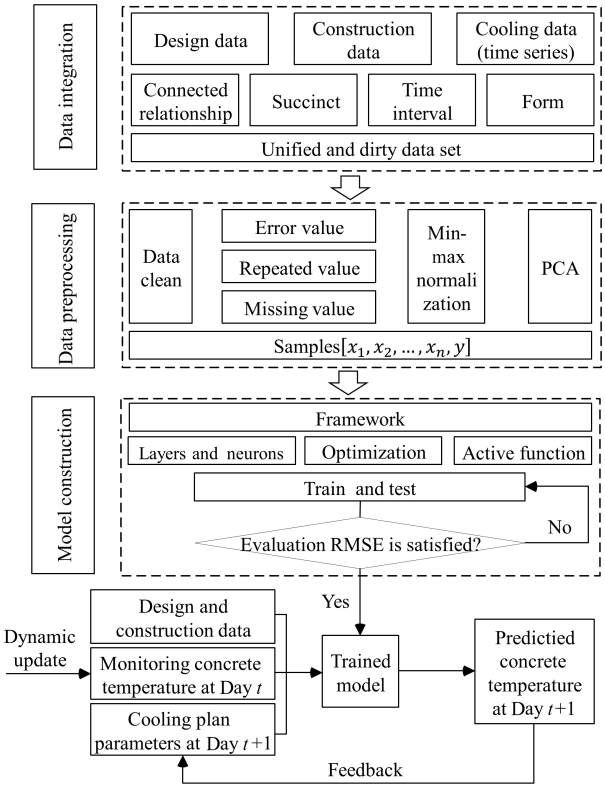

Fig. 1 Workflow of temperature prediction module.

(3) **Model construction.** The ANN framework is developed by iterative adjustment of model parameters until the loss function values reach the predefined tolerances. Quantities of ANN layers and neurons, optimization algorithms, and active functions are determined via sensitivity analysis. Samples are then divided into a training set and a test set. The forecast model is then trained and iteratively optimized until the loss function values are within the predefined tolerances, which are evaluated with RMSE.

With the trained forecast model, the concrete temperature at Day $t+1$ can be predicted using historical concrete cooling data from Day 1 to Day t. The predicted concrete temperature at Day $t+1$ can be compared with the relevant control requirements, and then feedback can be used to adjust the operation plan parameters at Day t. This process continues until the predicted temperature history of the concrete during placement and curing is within control requirements.

3.2 Data integration

In this study, concrete cooling-related data are collected through the ICCS. Input selection and forecast interval need to be determined before data collection. In developing this prediction model, 15 parameters related to concrete mix design, construction procedures, and cooling control operation are selected. For example, the parameter of concrete age (t_{age}) is selected to characterize the effect of hydration stage on concrete temperature. Features related to concrete block design are included to reflect different temperature evolution laws between varying concrete blocks. These features are block areas at the base (S_{block}), block thickness (h_{block}), placing time (t_{pour}), placing interval (I_{pour}), placing concrete volume (V_{conc_pour}), interval period (t_{inter}), design concrete volume (V_{conc_des}), concrete strength (σ_{conc}), concrete gradation (n_{grad}), and block elevation (H_{bottom}). Time series parameters of air temperature (T_{air}), average concrete temperature of a block (T_{conc}), inlet temperature (T_{water_in}), flow (Q_{water}), and other time series factors are also selected as input parameters.

A small prediction interval may not accurately reflect the impact of environmental changes, but a large prediction interval may result in ineffective temperature control. Considering hysteresis in the change of concrete temperature field, the forecast interval of one day is selected for the follow-up experiments in this study.

The raw monitoring data are distributed in Databases A through G, which require integration to form a standardized sample (Fig. 2). For non-time series data, the block number is used as the primary key (PK) in Databases A to D for connection. Time series data in Databases E and F are resampled by average at the interval of one day. Then time is used as PK, and block number is used as the foreign key for data integration to form a standardized dataset.

3.3 Data preprocessing

Data preprocessing aims to remove noises in the raw data and to meet the input requirements of completeness, consistency, and accuracy. The main tasks include data cleaning, normalization, and PCA.

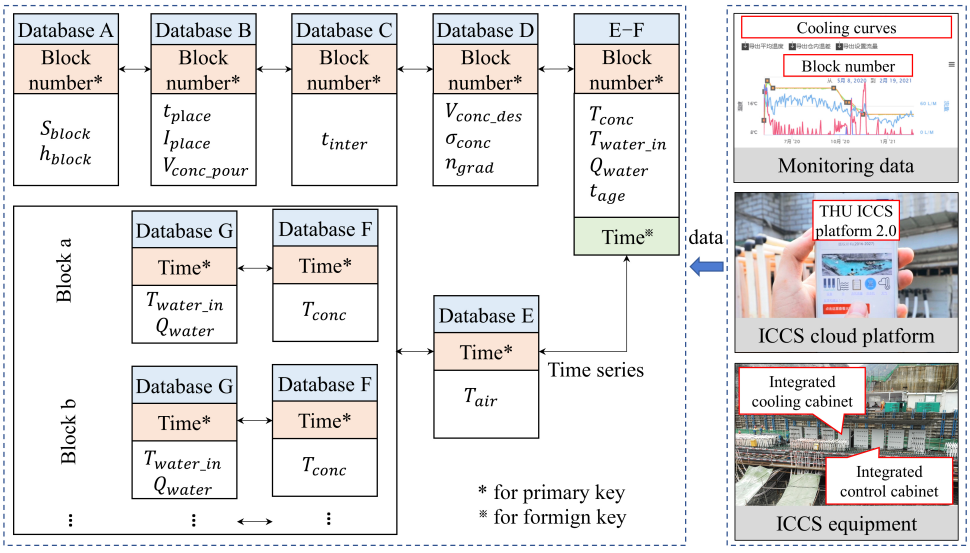

Fig. 2 Data integration from multiple sources.

(1) Data cleaning for temperature and flow series

Collected raw data are often mixed with various noises due to magnetic interference, power outages, long signal cables, sensor failure, and extreme construction environments. Data cleaning is carried out to deal with missing information or errors. Generally, time-series data, including T_{air}, T_{conc}, T_{water_in}, and Q_{water}, include more noise for large amounts and complex formats. Take data cleaning of T_{conc} as an example. Figure 3 shows the T_{conc} series of a block. This temperature data series has four typical types of noise as follows:

Noise 1: data collected before concrete placing. The sensor readings collect ambient temperature and not concrete temperature. In this study, Noise 1 is identified by checking the concrete temperature increases of the previous two days, Δt_0. Considering exothermic heat in early cement hydration stages, starting points may need adjustments when $\Delta t_0 < 2$ ℃.

Noise 2: missing temperature data. Missing values can be generated with linear interpretation.

Noise 3: excessively volatile temperature. This type of noise is within typical ranges and can be identified by abnormal fluctuations. Temperature change rates in adjacent days are adopted for screening Noise 3. Data are considered abnormal if the temperature change trends of consecutive two days are opposite (positive vs. negative) or if absolute values exceed the predefined limits. Excessive small range boundaries cause loss of correct data, though a smaller range boundary results in greater noise reduction. After reviewing the reduction effects of different ranges, the threshold is set at 0.3 ℃ for screening error values.

Noise 4: extreme temperature. Abnormal concrete temperature values (e.g., greater than 50 ℃ or less than 0 ℃) are removed and replaced as stated in Noise 2. By comparing concrete temperature series data between different blocks before and after cleaning, most of the noises are screened out successfully.

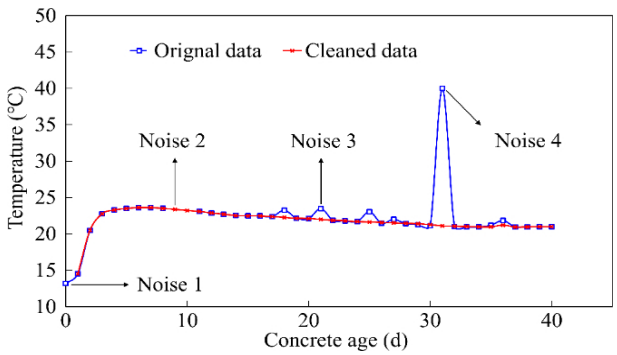

Fig. 3 Example of temperature data cleaning.

(2) Normalization

This process reduces the influence of the magnitude difference between varying parameters, improving convergence speed and model accuracy. T_{air} is typically less than 40 ℃, while V_{conc_pour} varies between 300 to 10 000 m^3. Normalization aims to map reading data to the same order of magnitude. Commonly-used normalization methods include min-max, z-score, and Sigmoid function. In this study, the min-max method is used to normalize the reading data:

$$x' = \frac{x - \text{MIN}}{\text{MAX} - \text{MIN}} \tag{1}$$

All input parameters are mapped into the range from zero to one (0, 1) after the min-max normalization.

(3) Principal component analysis

To deal with redundancy in model input parameters, we applied PCA to the normalized data. The development of the prediction model is simplified by removing redundant and irrelevant parameters in the input. The PCA transforms each column of data linearly and obtains multiple principal components sorted by the magnitudes of explained variances. The first n features are the primary contributors to the variances and are selected for model training, and the remaining dimensions are negligible and discarded. This process balances the model complexity and effective features.

3.4 Model construction

(1) Model framework

The proposed ANN-based forecast model is developed with two hidden layers. Figure 4 shows the framework. Design, construction, and cooling datasets are shaped as n-dimensional input vectors after data preprocessing. ANN then completes the information transfer from an n-dimensional input vector to a 1-dimensional output. The model contains a set of n-dimensional input vectors,

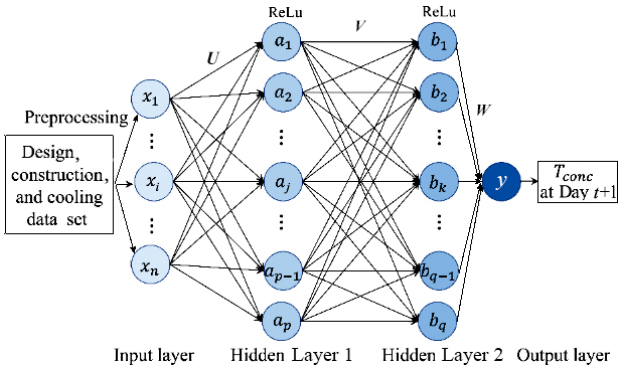

Fig. 4 Schematic framework of the ANN-based short-term temperature forecast model.

$\boldsymbol{X} = (x_1, x_2, \ldots, x_n)^{\mathrm{T}}$; Hidden Layer 1 of p neurons, $a_1, a_2, \ldots, a_p$; activation function, f_1; deviation of each neuron, α_j; Hidden Layer 2 of q neurons, $b_1, b_2, \ldots, b_q$; activation function, f_2; deviation of each neuron, β_j; output layer of 1 neuron with no activation function, y; and the neuron deviation, γ. In addition, the connection weights between Hidden Layer 1 and each node of the input layer are U_{ij}; between Hidden Layers 1 and 2 is V_{jk}; and between Hidden Layer 2 and each node of the output layer is W_k. Then, the output of Hidden Layer 1 neuron, a_j, is

$$a_j = f_1 \sum_{i=1}^{n} (x_i U_{ij} + \alpha_j), \quad j = 1, 2, \ldots, p \tag{2}$$

Similarly, the output of the Hidden Layer 2 neuron, b_k, is

$$b_k = f_2 \sum_{j=1}^{p} (a_j W_k + \beta_k), \quad k = 1, 2, \ldots, q \tag{3}$$

The model output value is

$$y = \sum_{k=1}^{q} b_k W_k + \gamma \tag{4}$$

The mapping of an n-dimensional input vector to a 1-dimensional output vector is completed via Eqs. (2)–(4), which is the forward propagation of neural information. The ANN model is trained via backward propagation, processing training samples for multiple iterations, and comparing the predicted and actual values of each sample. The loss function value in the current state of the neural network is assigned to each layer, and the connection weight of each neuron is adjusted accordingly. In general, when the model structure is appropriate, multiple training iterations can obtain a prediction model that meets the accuracy requirements.

(2) Regularization

To solve the over-fitting problem of the neural network model, we used the L1 regularization method. The L1 regularization norm is added to the objective functions to ensure that the values of the neural network parameters to be learned do not exceed the reasonable ranges. The L1 regularization is

$$L'(\theta) = L(\theta) + \lambda \sum_{i}^{n} |\theta_i| \tag{5}$$

where θ represents the network parameters to be learned, L' represents the loss function after introducing the regularization term, L represents the original loss function, and λ represents the L1 regularization coefficient.

(3) Activation function

The activation function enhances the nonlinear relationship between the input and output. For the hidden layers, rectified Linear Unit neurons (ReLU) are adopted. ReLU is the most widely used activation function in machine learning, expressed as

$$\mathrm{ReLU} = \max(0, x) \tag{6}$$

(4) Evaluation

Better neural network predictive modeling can be achieved by evaluating the obtained prediction model, adjusting the training parameters, and repeating this process until satisfactory results are obtained. In this study, the RMSE is used as the loss function for evaluation. By comparing the loss function values on the entire sample set, the most suitable network structure is constructed accordingly.

4 Case Study

The Baihetan Hydropower Station is being constructed and is to be completed in 2022. It is the world's second-largest hydropower station in electricity generation capacity, located on the mainstream of the Jinsha River in China. The Baihetan Dam is a concrete double-curved arch type, with a maximum height of 289 m and low-heat concrete usage of 8.03×10^6 m^3. Intelligent construction technologies such as the ICCS 2.0 are applied (Fig. 5). Thousands of sensors, including 6782

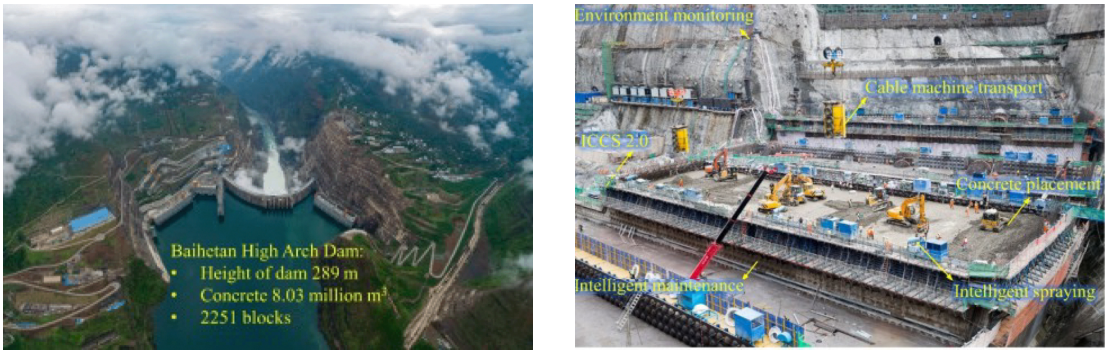

(a) Top view (b) Intelligent technologies used during dam construction

Fig. 5 Intelligent construction technologies of Baihetan high arch dam.

digital thermometers, are embedded in the dam to comprehensively monitor the construction.

4.1 Data for model training

Raw datasets used in data mining are collected by the ICCS 2.0. The types of data used after screening are summarized in Table 2.

Distribution characteristics of the dataset after data cleaning are explored. For temperature control of concrete blocks, the data include T_{air}, T_{water_in}, Q_{water}, t_{age}, and T_{conc}, represented by $(x_1, x_2, \ldots, x_4, x_5)$. Time-invariant data that characterize the differences between blocks include t_{inter}, σ_{conc}, n_{grad}, S_{block}, h_{block}, V_{conc_place}, t_{place}, I_{place}, I_{cable}, and H_{bottom}, represented by $(x_6, x_7, \ldots, x_{15})$. Single block data are regenerated as the average values of each block per day, yielding non-empty data of 92 184 samples. Data on multiple blocks are counted per block, yielding 349 samples with non-empty data.

Figure 6 shows the boxplot distributions of model input parameters. The median is represented by green lines, the upper and lower quartiles by blue lines, and the upper and lower bounds by gray lines. Boxplots of the sample data show that, in general, most parameters fall in the range 0–100. For example, T_{air} is 3.9–32.0 ℃ and T_{conc} is 7.5–28.0 ℃. Several parameters have small ranges, such as n_{grad} at 2.6–3.8, while others have greater variations, such as V_{conc_place} from 378.0–8848.5 m^3.

Table 2 Cooling-related parameters.

Source	Parameter considered
Design	Block number, S_{block}, h_{block}, V_{conc_des}, σ_{conc}, n_{grad}
Construction	V_{conc_place}, t_{place}, I_{place}, t_{inter}, I_{cable}
Cooling	T_{air}, T_{conc}, T_{water_in}, Q_{water}, t_{age}

4.2 Sample setting cutoff pair

The data require normalization to deal with wide magnitudes of parameters before its subsequent use as model input. Based on the selected 15 input parameters in Section 4.1, training samples are extracted from the integrated dataset. A total of 87 876 data samples from 346 concrete blocks are obtained after removing null values. The samples from the first 300 blocks are selected as the training set, while the remaining samples from 46 blocks are used for testing. Furthermore, 10% of the training set is selected for validation. The min-max normalization method is used to normalize the sample data. Table 3 shows Samples 1–5 after normalization.

Figure 7 shows the proportion of the explained variance of the 15 principal components after PCA transformation. The first 13 principal components account for 99.5% of the explained variance, while the 14th and 15th show relatively small explained variances. Further analysis of the principal component matrix shows that I_{cable} nearly only accounts for the 14th principal component. As a result, I_{cable} is considered as an irrelevant parameter and dropped from

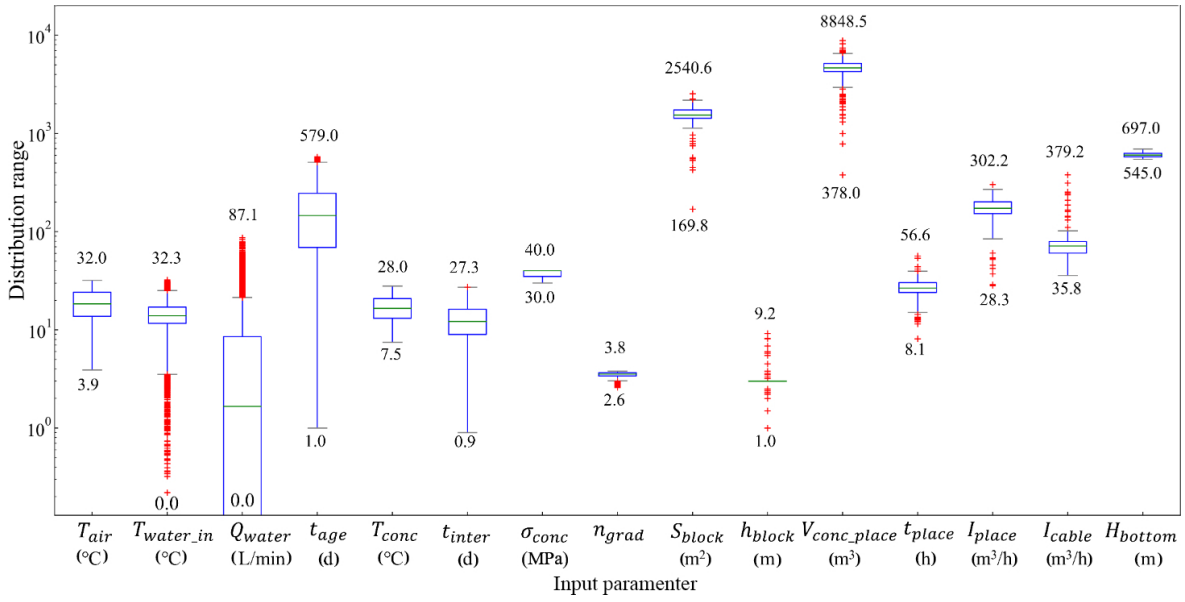

Fig. 6 Boxplot distribution of model input paramenters. The median is represented by green lines, the upper and lower quartiles by blue lines, and the upper and lower bounds by gray lines.

Table 3 Typical normalized samples of model input parameters.

T_{air} (℃)	T_{water_in} (℃)	Q_{water} (L·m^{-1})	t_{age} (d)	T_{conc} (℃)	t_{inter} (d)	σ_{conc} (MPa)	n_{grad}	S_{block} (m^3)	h_{block} (m)	V_{conc_place} (m^3)	t_{place} (h)	I_{place} (m^3·h^{-1})	I_{cable} (m^3·h^{-1})	H_{bottom} (m)
0.466	0.317	0.279	0.000	0.270	0.265	0.541	0.844	0.586	0.244	0.510	0.505	0.422	0.109	0.663
0.477	0.311	0.189	0.002	0.518	0.265	0.541	0.844	0.586	0.244	0.510	0.505	0.422	0.109	0.663
0.498	0.332	0.266	0.003	0.710	0.265	0.541	0.844	0.586	0.244	0.510	0.505	0.422	0.109	0.663
0.484	0.327	0.268	0.005	0.777	0.265	0.541	0.844	0.586	0.244	0.510	0.505	0.422	0.109	0.663
0.502	0.330	0.259	0.007	0.807	0.265	0.541	0.844	0.586	0.244	0.510	0.505	0.422	0.109	0.663

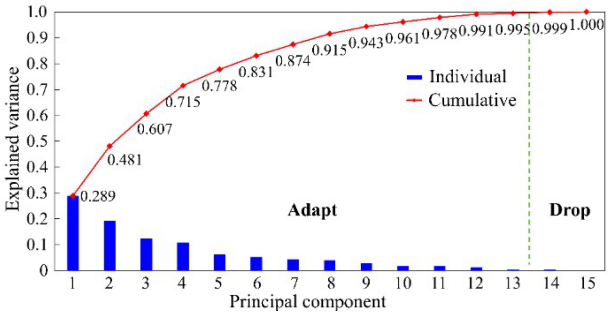

Fig. 7 PCA and explained variance of 15 parameters.

the input vector.

4.3 Model construction

The framework of the ANN model is explored for its activation function, quantities of hidden layers and neurons, and optimization algorithm. Given its good nonlinear function approximation, the ReLU function is adopted as the activation function of the ANN model. The RMSE in the test set is adopted as the index of accuracy evaluation for the framework optimization (Fig. 8). When the ANN framework has only one hidden layer, the RMSE of different neurons in the first layer is 0.35 ℃ (Fig. 8a). When the framework is set with two hidden layers, the RMSE of different neurons in the first and second layers generally concentrates at approximately 0.12 ℃ and can be divided into four regions (Fig. 8b). In Regions i, iii, and iv, the first and second layers have few neurons, resulting in poor learning ability. In Region ii, the neurons in the first layer are greater than 25, and the neurons in the second layer are greater than 10. Thus, the framework can obtain satisfying accuracy. The model containing two hidden layers with 28 and 15 neurons, respectively, is selected as the final framework.

As for optimization of the ANN-based forecast model training, six algorithms are introduced, including Adadelta, Adagrad, Adam, Nadam, RMSprop, and stochastic gradient descent (SGD) (Fig. 8c). Except for the SGD, the RMSEs of the training, validation, and test sets are similar, showing good generalization ability. Adam is a first-order optimization algorithm that can

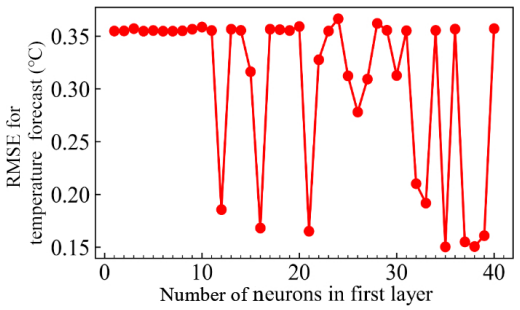

(a) With one hidden layer

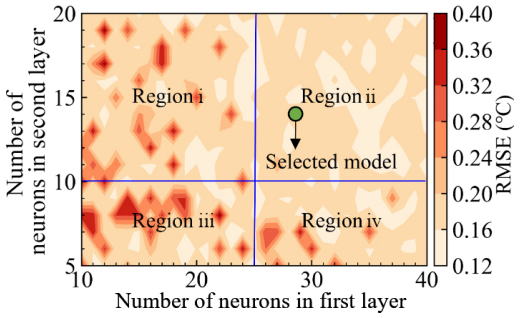

(b) With two hidden layers

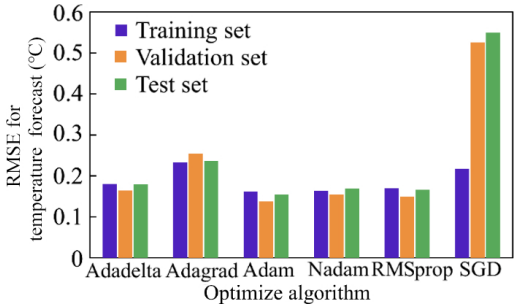

(c) Different optimization algorithms

Fig. 8 RMSE for concrete temperature forecast of ANN-based model with different framework structures.

replace the traditional SGD. Adam can update the weight of neural networks iteratively based on the training data and is found as the optimal algorithm with a minimum error of 0.14 ℃.

4.4 Forecast and discussion

Figure 9 shows the loss function of the ANN-based forecast model as measured with RMSE and mean absolute error (MAE). The loss function value reaches

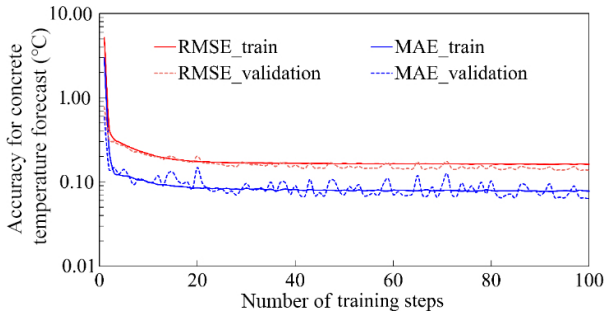

Fig. 9 Accuracy evaluation for concrete temperature forecast in ANN-based model training.

numerical convergence after 20 training iterations. To further improve the accuracy, we trained the final model with 100 iterations. The RMSE of the training set is 0.16 ℃, and that for the validation set is 0.14 ℃. The MAE of the training set is 0.08 ℃, and that for the validation set is 0.06 ℃. The results indicate that the ANN-based forecast model has high precision and does not fall into over-fitting.

To compare the effect of other machine learning algorithms on concrete temperature prediction, we also developed short-term forecast models based on SVM, LSTM, and DT. Figure 10 shows the prediction error distributions of these models. All models show stability on the training and test sets, although the ANN-based forecast model has higher precision than SVM, LSTM, and DT. For the ANN-based forecast model, 90% of prediction errors are within −0.13 to 0.12 ℃, and 98% of prediction errors are within −0.33 to 0.35 ℃.

The ANN-based forecast model is further evaluated by grouping the original cooling data by block and used in static one-step-ahead predictions. Figure 11 shows the prediction values and errors of eight typical blocks. Blocks a, b, c, and d are in the training set, whereas Blocks e, f, g, and h are in the test set. In general, the prediction error of the training set is significantly close to that of the test set, supporting the performance of the ANN-based short-term temperature forecast model.

Concrete age and cooling strategies are key influencing factors of the prediction error. (1) Concrete age. As for the cooling process, the prediction error shows different distributions before and after the maximum temperature, which is usually reached during 7–30 d after placement. During the temperature rise, the prediction error can be beyond ±1 ℃ (Blocks g and h), which is mainly less than ±0.2 ℃ during the cooling period. This error is reasonable and acceptable, considering the large temperature rises in the initial stage of placing. (2) Cooling strategy. Two kinds of mass concrete cooling strategies are used in the Baihetan Dam, namely, phased cooling (Blocks a and e) and continuous cooling (Blocks b and f). The prediction error of Blocks b and f is significantly less than that of Blocks a and e, indicating the advantages of the continuous cooling strategy with the development and application of an intelligent cooling control algorithm.

5 Conclusion

This study presents the development of an ANN-based short-term temperature forecast model for mass concrete cooling control. This model processes data on concrete design, construction, and cooling and then forecasts concrete temperatures at an interval of one day. The results can provide managers with accurate and real-time predictions on concrete temperature changes in a complex dam construction site. The key contributions of this study are as follows:

(1) The intelligent cooling control dataset is developed using multi-sources construction data through ICCS 2.0 in hydropower station projects. The workflow to develop the forecast model includes data integration, data preprocessing, model construction, and model

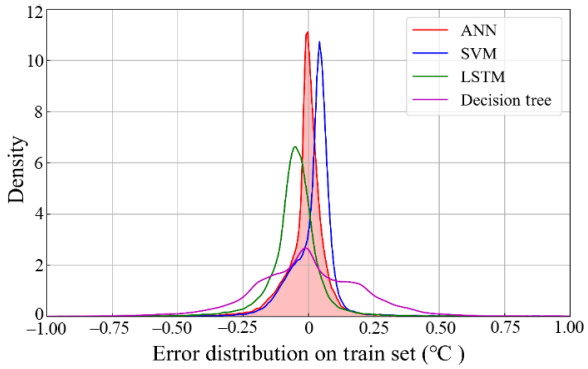

(a) Training set

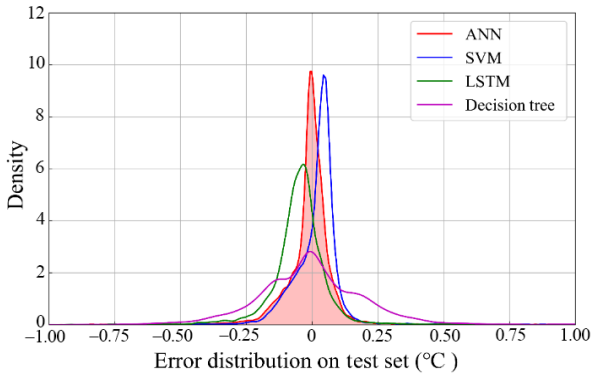

(b) Test set

Fig. 10 Prediction error density distribution of data mining algorithm.

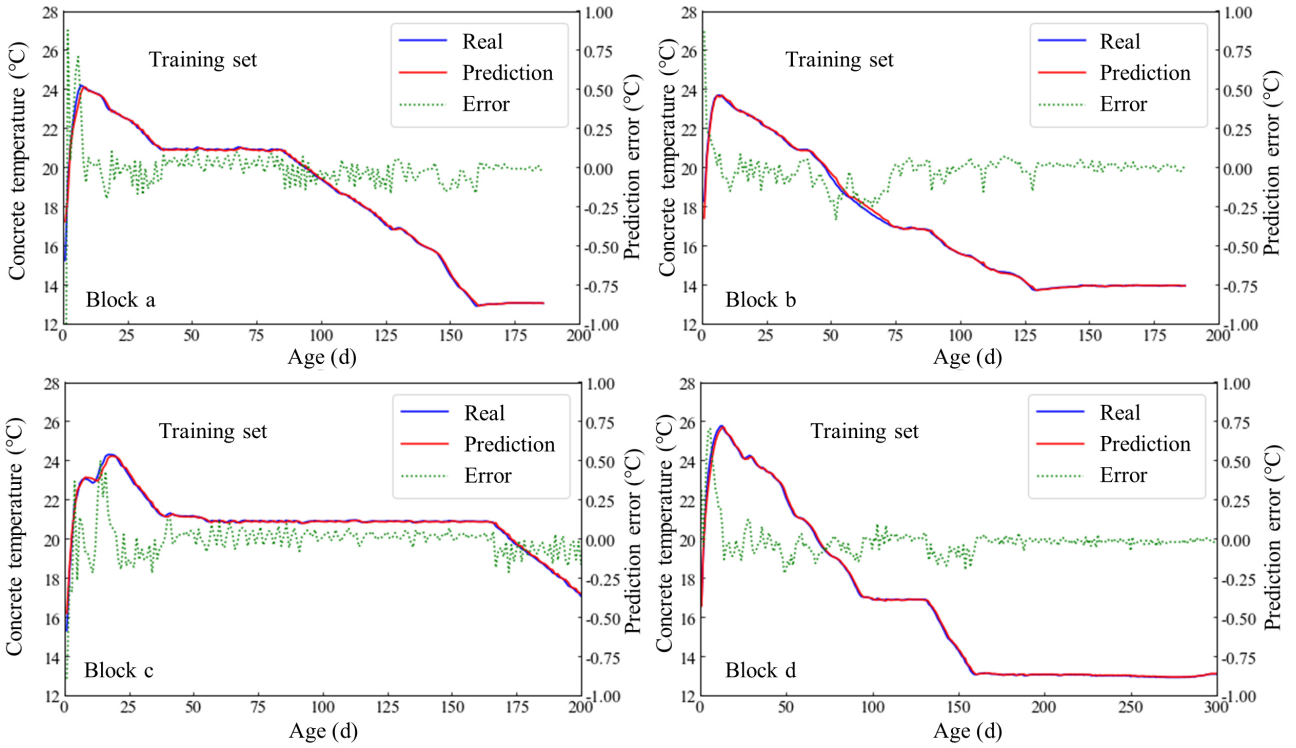

(a) Training set

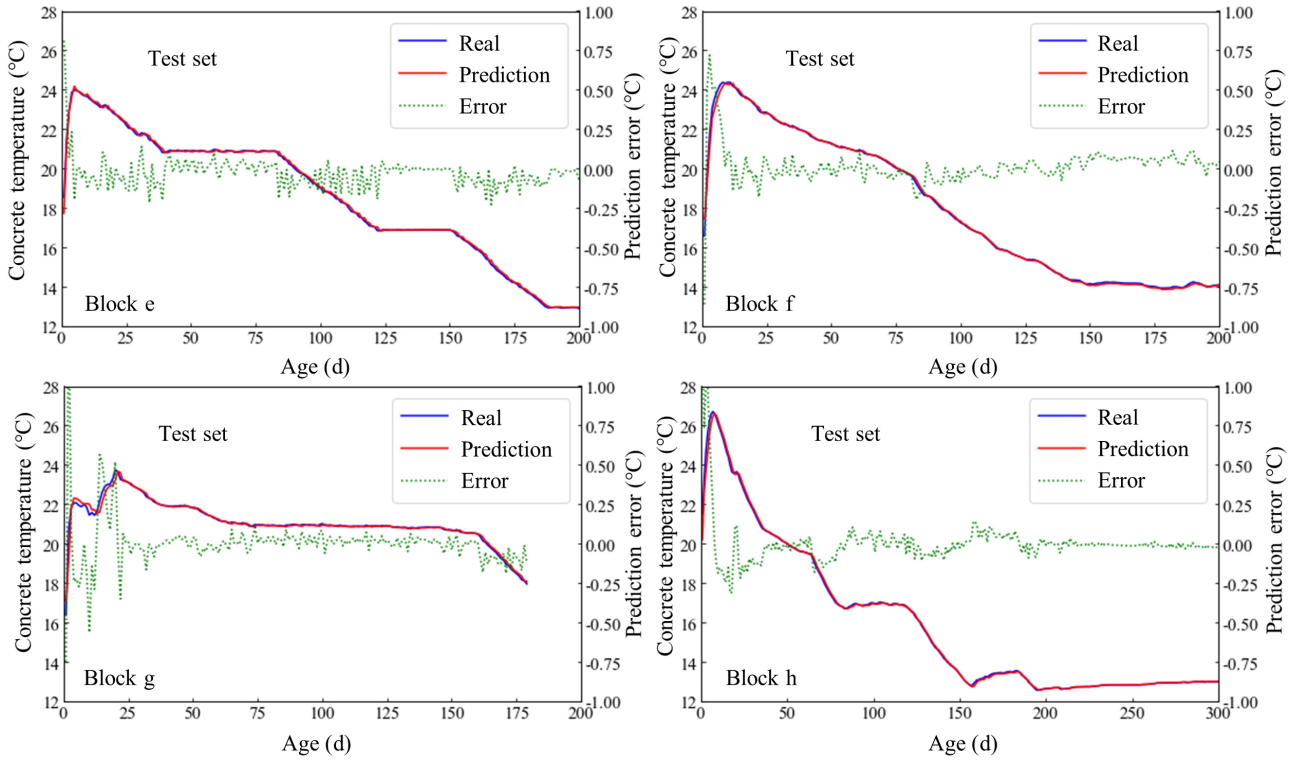

(b) Test set

Fig. 11 ANN-based model application on concrete blocks.

application.

(2) Temperature predictions of different machine learning algorithms are compared. The ANN was determined to be better than SVM, LSTM, and DT, showing the best prediction error distribution.

(3) An ANN-based short-term temperature forecast

model is developed and optimized with an RMSE of 0.15℃ on all 87 876 samples. The experimental application on concrete blocks verifies that the developed ANN-based forecast model can be used for intelligent cooling control during similar concrete construction projects.

The forecast model is implemented in the ICCS for concrete cooling control at the Baihetan Dam. Post-construction investigation indicates no thermal cracks in the concrete blocks.

Acknowledgment

This research was supported by the China Three Gorges Corporation Research Program (Nos. WDD/0490, WDD/0578, and BHT/0805) and the National Natural Science Foundation of China (No. 51979146).

References

[1] P. Lin, W. Y. Zhou, and H. Y. Liu, Experimental study on cracking, reinforcement, and overall stability of the Xiaowan super-high arch dam, *Rock Mech. Rock Eng.*, vol. 48, no. 2, pp. 819–841, 2015.

[2] J. Shi, P. Lin, Y. D. Zhou, P. C. Wei, and R. K. Wang, Reinforcement analysis of toe blocks and anchor cables at the Xiluodu super-high arch dam, *Rock Mech. Rock Eng.*, vol. 51, no. 8, pp. 2533–2554, 2018.

[3] P. Lin, X. X. Zhu, Q. B. Li, H. Y. Liu, and Y. J. Yu, Study on optimal grouting timing for controlling uplift deformation of a super high arch dam, *Rock Mech. Rock Eng.*, vol. 49, no. 1, pp. 115–142, 2016.

[4] J. D. Xin, G. X. Zhang, Y. Liu, Z. H. Wang, N. Yang, Y. F. Wang, R. F. Mou, Y. Qiao, J. Wang, and Z. Wu, Environmental impact and thermal cracking resistance of low heat cement (LHC) and moderate heat cement (MHC) concrete at early ages, *J. Build. Eng.*, vol. 32, p. 101668, 2020.

[5] Z. H. Wang, Y. Liu, G. X. Zhang, and W. Q. Hou, Schematic study on temperature control and crack prevention during spillway tunnel concreting period, *Mater. Struct.*, vol. 48, no. 11, pp. 3517–3525, 2015.

[6] P. Lin, Q. B. Li, and H. Hu, A flexible network structure for temperature monitoring of a super high arch dam, *Int. J. Distrib. Sens. Netw.*, vol. 2012, no. 11, p. 917849, 2012.

[7] P. Lin, Q. X. Fan, Z. L. Wang, W. F. Chen, Z. L. Yang, and S. W. Zhou, Intelligent control system and method for medium heat exchange, (in Chinese), CN110006284B, May 15, 2020.

[8] Q. L. Zhang, Z. Z. An, T. Y. Liu, Z. S. Zhang, Z. H. Huangfu, Q. B. Li, Q. J. Yang, and J. Q. Liu, Intelligent rolling compaction system for earth-rock dams, *Autom. Constr.*, vol. 116, p. 103246, 2020.

[9] P. Lin, H. Y. Peng, Q. X. Fan, Y. F. Xiang, Z. L. Yang, and N. Yang, A 3D thermal field restructuring method for concrete dams based on real-time temperature monitoring, *KSCE J. Civil Eng.*, vol. 25, no. 4, pp. 1326–1340, 2021.

[10] H. Z. Su, X. Li, B. B. Yang, and Z. P. Wen, Wavelet support vector machine-based prediction model of dam deformation, *Mech. Syst. Signal Process.*, vol. 110, pp. 412–427, 2018.

[11] Y. Su, K. L. Weng, C. Lin, and Z. Q. Chen, Dam deformation interpretation and prediction based on a long short-term memory model coupled with an attention mechanism, *Appl. Sci.*, vol. 11, no. 14, p. 6625, 2021.

[12] B. K. Oh, H. S. Park, and B. Glisic, Prediction of long-term strain in concrete structure using convolutional neural networks, air temperature and time stamp of measurements, *Autom. Constr.*, vol. 126, p. 103665, 2021.

[13] S. Y. Chen, C. S. Gu, C. N. Lin, Y. Wang, and M. A. Hariri-Ardebili, Prediction, monitoring, and interpretation of dam leakage flow via adaptative kernel extreme learning machine, *Measurement*, vol. 166, p. 108161, 2020.

[14] W. S. Song, T. Guan, B. Y. Ren, J. Yu, J. J. Wang, and B. P. Wu, Real-time construction simulation coupling a concrete temperature field interval prediction model with optimized hybrid-kernel RVM for arch dams, *Energies*, vol. 13, no. 17, p. 4487, 2020.

[15] H. Y. Xie, W. Shi, R. R. A. Issa, X. T. Guo, Y. Shi, and X. J. Liu, Machine learning of concrete temperature development for quality control of field curing, *J. Comput. Civil Eng.*, vol. 34, no. 5, p. 04020031, 2020.

[16] B. Liu, S. Yan, H. L. You, Y. Dong, Y. Li, J. L. Lang, and R. T. Gu, Road surface temperature prediction based on gradient extreme learning machine boosting, *Comput Ind.*, vol. 99, pp. 294–302, 2018.

[17] Q. X. Fan, P. Lin, P. C. Wei, Z. Y. Ning, and G. Li, Closed-loop control theory of Intelligent construction, (in Chinese), *J. Tsinghua Univ. (Sci. Technol.)*, vol. 61, no. 7, pp. 660–670, 2021.

[18] H. W. Zhou, Y. H. Zhou, C. J. Zhao, F. Wang, and Z. P. Liang, Feedback design of temperature control measures for concrete dams based on real-time temperature monitoring and construction process simulation, *KSCE J. Civil Eng.*, vol. 22, no. 5, pp. 1584–1592, 2018.

[19] D. H. Zhong, M. N. Shi, B. Cui, J. J. Wang, and T. Guan, Research progress of the intelligent construction of dams, (in Chinese), *J. Hydraul. Eng.*, vol. 50, no. 1, pp. 38–52&61, 2019.

[20] A. R. Ingraffea, H. N. Linsbauer, and H. P. Rossmanith, Computer simulation of cracking in a large arch dam downstream side cracking, in *Proc. SEM-RILEM Int. Conf. on Fracture of Concrete and Rock*, Houston, TX, USA, 1989, pp. 334–342.

[21] W. M. Wang, J. X. Ding, G. J. Wang, L. C. Zou, and S. H. Chen, Stability analysis of the temperature cracks in Xiaowan arch dam, *Sci. China Technol. Sci.*, vol. 54, no. 3, pp. 547–555, 2011.

[22] P. H. Burgi, 75 years of hydraulic investigations-hoover dam, in *Proc.*75^{th} *Anniversary History Symp.*, Las Vegas, NV, USA, 2010, pp. 249–266.

[23] M. Wieland, Q. Ren, and J. S. Y. Tan, eds, *New Developments in Dam Engineering*: *Proceedings of the 4th International Conference on Dam Engineering*, *18–20 October*, *Nanjing*, *China*. London, UK: CRC Press, 2004.

[24] N. Aniskin, C. N. Trong, and L. H. Quoc, Influence of size and construction schedule of massive concrete structures

on its temperature regime, *MATEC Web Conf.*, vol. 251, p. 02014, 2018.
[25] X. H. Liu, C. Zhang, X. L. Chang, W. Zhou, Y. G. Cheng, and Y. Duan, Precise simulation analysis of the thermal field in mass concrete with a pipe water cooling system, *Appl. Therm. Eng.*, vol. 78, pp. 449–459, 2015.
[26] A. Tasri and A. Susilawati, Effect of material of post-cooling pipes on temperature and thermal stress in mass concrete, *Structures*, vol. 20, pp. 204–212, 2019.
[27] T. A. Do, T. T. Hoang, T. Bui-Tien, H. V. Hoang, T. D. Do, and P. A. Nguyen, Evaluation of heat of hydration, temperature evolution and thermal cracking risk in high-strength concrete at early ages, *Case Stud. Therm. Eng.*, vol. 21, p. 100658, 2020.
[28] Z. Z. Zhang, Q. C. Xin, and F. Zhang, Impact of wind speed on temperature field of massive concrete at different air temperatures, (in Chinese), *Water Resour. Power*, vol. 33, no. 5, pp. 109–112, 2015.
[29] P. Lin, Q. B. Li, and P. Y. Jia, A real-time temperature data transmission approach for intelligent cooling control of mass concrete, *Math. Probl. Eng.*, vol. 2014, p. 514606, 2014.
[30] P. Lin, P. C. Wei, H. Y. Peng, Z. Y. Ning, and M. Li, Medium-based intelligent temperature control data management system and method, (in Chinese), CN109917831A, June 21, 2019.
[31] P. Lin, Z. Y. Ning, H. Y. Peng, and P. C. Wei, Mass concrete temperature control method based on intelligent learning, (in Chinese), CN109976147A, July 5, 2019.
[32] Z. Y. Zhu, Y. Liu, G. X. Zhang, C. C. Wu, Z. H. Wang, Y. Z. Liu, L. Zhang, and N. Yang, Micro-scale FEM calculation of concrete temperature during production and casting, *J. Wuhan Univ. Technol.-Mater. Sci. Ed.*, vol. 35, no. 1, pp. 113–120, 2020.
[33] C. Ponce-Farfán, D. Santillán, and M. Á. Toledo, Thermal simulation of rolled concrete dams: Influence of the hydration model and the environmental actions on the thermal field, *Water*, vol. 12, no. 3, p. 858, 2020.
[34] M. Zhang, X. H. Yao, J. F. Guan, and L. L. Li, Study on temperature field massive concrete in early age based on temperature influence factor, *Adv. Civil Eng.*, vol. 2020, pp. 8878974, 2020.
[35] T. C. Nguyen, T. S. Nguyen, Q. Van Nguyen, and T. M. D. Do, Finite element analysis of temperature and stress fields in the concrete mass with pipe-cooling, *Struct. Integr. Life*, vol. 20, no. 2, pp. 131–135, 2020.
[36] Y. Li, L. Nie, and B. Wang, A numerical simulation of thetemperature cracking propagation process when pouring mass concrete, *Autom. Constr.*, vol. 37, pp. 203–210, 2014.
[37] G. An, N. Yang, Q. B. Li, Y. Hu, and H. T. Yang, A simplified method for real-time prediction of temperature in mass concrete at early age, *Appl. Sci.*, vol. 10, no. 13, p. 4451, 2020.
[38] Y. H. A. Aziz, Y. A. Zaher, M. A. Wahab, and M. Khalaf, Predicting temperature rise in Jacketed concrete beams subjected to elevated temperatures, *Constr. Build. Mater.*, vol. 227, p. 116460, 2019.
[39] Y. J. Bie, S. Qiang, X. Sun, and J. D. Song, A new formula to estimate final temperature rise of concrete considering ultimate hydration based on equivalent age, *Constr. Build. Mater.*, vol. 142, pp. 514–520, 2017.
[40] J. Liu, Y. J. Liu, G. J. Zhang, L. Jiang, and X. K. Yan, Prediction formula for temperature gradient of concrete-filled steel tubular member with an arbitrary inclination, *J. Bridge Eng.*, vol. 25, no. 10, p. 04020076, 2020.
[41] A. Eymen and Ü. Köylü, Seasonal trend analysis and ARIMA modeling of relative humidity and wind speed time series around Yamula Dam, *Meteor. Atmos. Phys.*, vol. 131, no. 3, pp. 601–612, 2019.
[42] S. Y. Hou, W. G. Li, T. Y. Liu, S. G. Zhou, J. H. Guan, R. F. Qin, and Z. F. Wang, D2CL: A dense dilated convolutional LSTM model for sea surface temperature prediction, *IEEE J. Sel. Top. Appl. Earth Obs. Remote Sens.*, vol. 14, pp. 12514–12523, 2021.
[43] J. Li, Rapid prediction on temperature of concrete in the concreting process based on GA-SVM, (in Chinese), Master dissertation, Tsinghua University, Beijing, China, 2016.
[44] I. E. Livieris, E. Pintelas, and P. Pintelas, A CNN-LSTM model for gold price time-series forecasting, *Neural Comput. Appl.*, vol. 32, no. 23, pp. 17351–17360, 2020.
[45] H. X. Zang, L. Liu, L. Sun, L. L. Cheng, Z. N. Wei, and G. Q. Sun, Short-term global horizontal irradiance forecasting based on a hybrid CNN-LSTM model with spatiotemporal correlations, *Renew. Energy*, vol. 160, pp. 26–41, 2020.
[46] C. Z. Zhang, F. H. Zhu, X. Wang, L. L. Sun, H. N. Tang, and Y. S. Lv, Taxi demand prediction using parallel multi-task learning model, *IEEE Trans. Intell. Transp. Syst.*, vol. 23, no. 2, pp. 794–803, 2022.
[47] P. G. Asteris, A. D. Skentou, A. Bardhan, P. Samui, and K. Pilakoutas, Predicting concrete compressive strength using hybrid ensembling of surrogate machine learning models, *Cem. Concr. Res.*, vol. 145, p. 106449, 2021.
[48] X. Y. Cai, Rapid analysis and prediction on temperature of dam in the concreting process based on data mining, (in Chinese), Master dissertation, Tsinghua University, Beijing, China, 2015.

Peng Lin received the BS, MSc, and PhD degrees from Northeastern University, Shenyang, China, in 1995, 1998, and 2002, respectively. He has worked as a professor at the Department of Hydraulic Engineering, Tsinghua University, Beijing, China, since 2014. His research interests include intelligent construction, dam cracking control, and rock mecheansim and engineering.

Ming Li received the BSc degree in hydraulic engineering from Tsinghua University, Beijing, China, in 2019. He is currently pursuing the PhD degree in hydraulic engineering at Tsinghua University, Beijing, China. His research interests mainly include dam intelligent construction and cooling control.

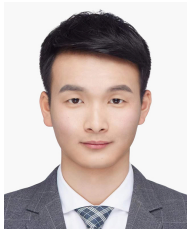

Daoxiang Chen received the BSc degree in hydraulic engineering from Tsinghua University, Beijing, China, in 2021. He is currently pursuing the PhD degree in hydraulic engineering at the Department of Hydraulic Engineering, Tsinghua University, Beijing, China. His research interests mainly include intelligent dam construction and vibroflotation method.

Zichang Li received the BSc and MSc degrees in hydraulic engineering from Tsinghua University, Beijing, China, in 2008 and 2010, respectively, and the PhD degree in civil and environmental engineering from the University of Pittsburgh, Pittsburgh, USA, in 2015. He is currently working at the Sichuan Energy Internet Research Institute, Tsinghua University, Chengdu, China. His research interests include geotechnical analyses and intelligent technologies for infrastructure construction.

Ke Liu received the BSc degree from Sichuan University, Chengdu, China, in 2007. He is currently working at China Three Gorges Construction Engineering Corporation, Chengdu, China. His research interests include dam construction and management.

Yaosheng Tan received the PhD degree in hydraulic engineering from Tianjin University, Tianjin, China, in 2015. He is currently working at China Three Gorges Construction Engineering Corporation, Chengdu, China. His research interests include dam construction and management.